

Langmuir–Blodgett Films of Regioregular Poly(3-hexylthiophene) as Field-Effect Transistors

Guofeng Xu,[†] Zhenan Bao,[‡] and John T. Groves^{*,†}

Department of Chemistry, Princeton University, Princeton, New Jersey 08544

Received April 13, 1999. In Final Form: September 23, 1999

The application of Langmuir–Blodgett (LB) techniques to conjugated polymers offers a unique approach for constructing molecular devices. In this paper, we made thin film field-effect transistors (FET) by LB techniques, based on regioregular poly(3-hexylthiophene) (RR–PHT). Langmuir films of RR–PHT were stable at the air–water interface and could be transferred onto hydrophobic substrates by horizontal deposition. The LB films prepared from three different methods were characterized by UV–Vis absorption spectroscopy, polarized visible absorption, X-ray diffraction, reflective absorption IR spectroscopy, and field-effect mobility. The field-effect mobility of these FETs were among the highest of polymeric thin film LB FET devices.

Introduction

Langmuir–Blodgett (LB) techniques offer a unique approach to prepare ordered ultrathin films with well-defined architecture,^{1–3} thus providing a promising and versatile method for constructing molecular devices.^{4–7} Conjugated polymers have drawn intense research interest as active materials for such devices, due to their unusual electrical and optical properties, reasonable chemical stability, and easy processability.^{8–25} The application of the LB technique to conjugated polymers has produced a variety of electrical and optical ultrathin film

devices, such as light emitting diodes (LED),^{26–31} thin film conductors,^{32–36} memory devices,³⁷ ferroelectric thin films,^{38–41} nonlinear optical devices,^{42–44} sensors^{45–49} and field-effect transistors (FET).^{50,51}

[†] Bell Laboratories, Lucent Technologies 600 Mountain Avenue, Murray Hill, New Jersey 07974-0636.

- (1) Roberts, G. *Langmuir–Blodgett Films*; Plenum: New York, 1990.
 (2) Wegner, G. *Thin Solid Films* **1992**, *216*, 105.
 (3) Esker, A. R.; Mengel, C.; Wegner, G. *Science* **1998**, *280*, 892.
 (4) Birge, R. R. *Molecular and Biomolecular Electronics*; American Chemical Society: Washington, DC, 1994; Vol. 240.
 (5) Aizawa, M.; Nishiguchi, K.; Imamura, M.; Kobatake, E.; Haruyama, T.; Ikariyama, Y. *Sensors and Actuators B* **1995**, *24*, 1.
 (6) Nicolini, C.; Adami, M.; Dubrovsky, T.; Erokhin, V.; Facci, P.; Paschkevitch, P.; Sartore, M. *Sensors and Actuators B* **1995**, *24*, 121.
 (7) Nicolini, C. *Thin Solid Films* **1996**, *285*, 1.
 (8) Heeger, A. J. *Rev. Mod. Phys.* **1988**, *60*, 781.
 (9) Burroughes, J. H.; Jones, C. A.; Friend, R. H. *Nature* **1988**, *335*, 137.
 (10) Yassar, A.; Roncali, J.; Garnier, F. *Macromolecules* **1989**, *22*, 804.
 (11) Yang, Y.; Heeger, A. J. *Nature* **1994**, *372*, 344.
 (12) Bredas, J. L.; Adant, C.; Tackx, P.; Persoons, A.; Pierce, B. M. *Chem. Rev.* **1994**, *94*, 243.
 (13) Bakhshi, A. K. *Bull. Materials Sci.* **1995**, *18*, 469.
 (14) Pei, Q.; Yu, G.; Zhang, C.; Yang, Y.; Heeger, A. J. *Science* **1995**, *269*, 1086.
 (15) Weaver, M. S.; Lidzey, D. G.; Fisher, T. A.; Pate, M. A.; Bleyer, A.; Tajbakhsh, A.; Bradley, D. D. C.; Skolnick, M. S.; Hill, G. *Thin Solid Films* **1996**, *273*, 39.
 (16) Feast, W. J.; Tsibouklis, J.; Pouwer, K. L.; Groenendaal, L.; Meijer, E. W. *Polymer* **1996**, *37*, 5017.
 (17) Rothberg, L. J.; Lovinger, A. J. *J. Mater. Res.* **1996**, *11*, 3174.
 (18) Yu, G.; Heeger, A. J. *Synthetic Metals* **1997**, *85*, 1183.
 (19) Dodabalapur, A. *Solid State Commun.* **1997**, *102*, 259.
 (20) Rothberg, L. J.; Yan, M.; Kwock, E. W.; Miller, T. M.; Galvin, M. E.; Son, S.; Papadimitrakopoulos, F. *IEEE-Trans. Electron Devices* **1997**, *44*, 1258.
 (21) Higgins, S. J. *Chem. Soc. Rev.* **1997**, *26*, 247.
 (22) Hide, F.; Schwartz, B. J.; DiazGarcia, M. A.; Heeger, A. J. *Synth. Metals* **1997**, *91*, 35.
 (23) Brown, A. R.; Jarrett, C. P.; deLeeuw, D. M.; Matters, M. *Synth. Metals* **1997**, *88*, 37.
 (24) Drury, C. J.; Mutsaers, M. J.; Hart, C. M.; Matters, M.; de Leeuw, D. M. *Appl. Phys. Lett.* **1998**, *73*, 108.
 (25) Dodabalapur, A.; Bao, Z.; Makhija, A.; Laquindanum, J. G.; Raju, V. R.; Feng, Y.; Katz, H. E.; Rogers, J. *Appl. Phys. Lett.* **1998**, *73*, 142.

- (26) Wu, A. P.; Kakimoto, M. A. *Adv. Mater.* **1995**, *7*, 812.
 (27) Wu, A. P.; Akagi, T.; Jikei, M.; Kakimoto, M.; Imai, Y.; Ukishima, S.; Takahashi, Y. *Thin Solid Films* **1996**, *273*, 214.
 (28) Cimrova, V.; Remmers, M.; Neher, D.; Wegner, G. *Adv. Mater.* **1996**, *8*, 146.
 (29) Pal, A. J.; Ostergard, T.; Paloheimo, J.; Stubb, H. *Appl. Phys. Lett.* **1996**, *69*, 1137.
 (30) Ostergard, T.; Paloheimo, J.; Pal, A. J.; Stubb, H. *Synth. Metals* **1997**, *88*, 171.
 (31) DonatBouillud, A.; Mazerolle, L.; Gagnon, P.; Goldenberg, L.; Petty, M. C.; Leclerc, M. *Chem. Materials* **1997**, *9*, 2815.
 (32) Ando, M.; Watanabe, Y.; Iyoda, T.; Honda, K.; Shimidzu, T. *Thin Solid Films* **1989**, *179*, 225.
 (33) Rikukawa, M.; Nakagawa, M.; Abe, H.; Ishida, K.; Sanui, K.; Ogata, N. *Thin Solid Films* **1996**, *273*, 240.
 (34) Park, Y. H.; Park, S. Y.; Nam, S. W.; Park, C. R.; Kim, Y. J. *J. Appl. Polym. Sci.* **1996**, *60*, 865.
 (35) Granholm, P.; Paloheimo, J.; Stubb, H. *Synth. Metals* **1997**, *84*, 783.
 (36) Paddeu, S.; Ram, M. K.; Nicolini, C. *J. Phys. Chem. B* **1997**, *101*, 4759.
 (37) Takimoto, K.; Kuroda, R.; Shido, S.; Yasuda, S.; Matsuda, H.; Eguchi, K.; Nakagiri, T. *J. Vacuum Sci. Technol. B* **1997**, *15*, 1429.
 (38) Palto, S.; Blinov, L.; Bune, A.; Dubovik, E.; Fridkin, V.; Petukhova, N.; Verkhova, K.; Yudin, S. *Ferroelectrics Lett.* **1995**, *19*, 65.
 (39) Xue, Q. B.; Chen, X.; Yang, K. Z.; Zhang, Q. Z. *Macromol. Chem. Phys.* **1995**, *196*, 3243.
 (40) Blinov, L. M.; Fridkin, V.; Palto, S. P.; Sorokin, A. V.; Yudin, S. G. *Thin Solid Films* **1996**, *285*, 474.
 (41) Bune, A. V.; Fridkin, V. M.; Ducharme, S.; Blinov, L. M.; Palto, S. P.; Sorokin, A. V.; Yudin, S. G.; Zlatkin, A. *Nature* **1998**, *391*, 874.
 (42) Wijekoon, W. M. K. P.; Wilaya, S. K.; Bhawalkar, J. D.; Prasad, P. N.; Penner, T. L.; Armstrong, N. J.; Williams, D. J. *J. Am. Chem. Soc.* **1996**, *118*, 4480.
 (43) Nguyen, D. M.; Mayer, T. M.; Hubbard, S. F.; Singer, K. D.; Mann, J. A.; Lando, J. B. *Macromolecules* **1997**, *30*, 6150.
 (44) Jung, C.; Jikei, M.; Kakimoto, M. *J. Optical Soc. Am. B* **1998**, *15*, 471.
 (45) Schoning, M. J.; Sauke, M.; Steffen, A.; Marso, M.; Kordos, P.; Luth, H.; Kauffmann, F.; Erbach, R.; Hoffmann, B. *Sensors and Actuators B* **1995**, *27*, 325.
 (46) Agbor, A. E.; Petty, M. C.; Monkman, A. P. *Sensors and Actuators B* **1995**, *28*, 173.
 (47) Millella, E.; Musio, F.; Alba, M. B. *Thin Solid Films* **1996**, *285*, 908.
 (48) Lavrik, N. V.; DeRossi, D.; Kazantseva, Z. I.; Nabok, A. V.; Nesterenko, B. A.; Piletsky, S. A.; Kalchenko, V. I.; Shivaniuk, A. N.; Markovskiy, L. N. *Nanotechnology* **1996**, *7*, 315.
 (49) Ng, S. C.; Zhou, X. C.; Chen, Z. K.; Miao, P.; Chan, H. S. O.; Li, S. F. Y.; Fu, P. *Langmuir* **1998**, *14*, 1748.
 (50) Paloheimo, J.; Kuivalainen, P.; Stubb, H.; Vuorimaa, E.; Yli-Lahti, P. *Appl. Phys. Lett.* **1990**, *56*, 1157.

The first LB field-effect transistors made of conjugated polymer semiconductors were reported by Paloheimo et al.,⁵⁰ using regiorandom poly(3-alkylthiophene) as the active material. However, these LB FET devices showed very low charge carrier mobility, typically in the range of 10^{-7} to 10^{-4} cm² V⁻¹ s⁻¹.⁵⁰⁻⁵² The low field-effect mobility was due to a number of reasons: First, the active materials used in these cases were regioirregular poly(3-alkylthiophenes) (RI-PAT), in which alkyl side chains were randomly placed along the polymer backbone. The steric hindrance caused by this type of side chain arrangement prevented polymers from effective conjugating and ordered π - π stacking, leading to a low charge carrier mobility.⁵³ Second, RI-PATs could not form stable and transferable films at the air/water interface unless long chain fatty acids were added in large amounts to form a supporting matrix.^{50,51,54,55} This, however, led to further complications: 1. The presence of long chain fatty acids (usually, a nonconducting substance) dramatically reduced the charge carrier mobility of the films;^{50,55} 2. PATs had rather random conformations and orientations within the fatty acid matrix;⁵⁵ 3. Devices usually had a short lifetime due to the inherent instability of fatty acid LB films, which often resulted in a complete destruction of the layered structure.^{2,29} Therefore, FETs made of pure conjugated polymers are still needed for constructing high performance stable thin film devices.

Recently, thin film FETs with high mobility have been successfully made by solution methods with regioregular poly(3-hexylthiophene) (RR-PHT).⁵⁶ These polymers can be synthesized using methods developed by McCullough et al.^{53,57,58} and others.^{59,60} Due to an enhanced conjugation between thiophene rings and a better ordering in the solid state,⁵³ regioregular PATs (RR-PATs) have demonstrated much better electrical and optical properties than their regiorandom counterparts. In addition, RR-PATs are much more likely than RI-PATs to form stable Langmuir films. The high degree of coplanarity along the backbones of RR-PAT enables an effective intermolecular stacking, which facilitates the formation of a lamella supramolecular assembly or a well-ordered rodlike structure.^{53,57,58,61} Polymers with a hairy-rodlike structure have shown the ability to form stable and transferable Langmuir films despite the lack of an apparent amphiphilicity.² Given their structural similarity to hairy-rod polymers, RR-PATs are also likely to form stable Langmuir films.⁶²

In light of these recent technology advances, we explore the possibility of fabricating ultrathin film devices of field-effect transistors, by applying Langmuir-Blodgett techniques to pure regioregular poly(3-hexylthiophene) (RR-PHT). The field-effect mobility is used as one parameter to probe the molecular ordering in these LB films. Herein,

we describe the fabrication of LB RR-PHT films by three different methods and the comparative characterization of their physical properties, such as surface pressure-area isotherms, spectroscopic and structural characteristics, and field-effect mobility.

Experimental Section

PHT was synthesized following the procedure described previously.⁵⁶ 1-dodecanol (puriss, Fluka), spectrophotometric grade chloroform (EM), methanol (EM), hexadecane (99+%, Aldrich), octadecyltrichlorosilane (95% Aldrich), carbon tetrachloride (99.9%, Aldrich) and xylene mixture (with boiling point range 137–144 °C, EM) were used as obtained.

The surface films were spread onto pure Milli-Q water subphase from corresponding spreading solutions: 0.25 mg/mL chloroform solution for type I films, 0.25 mg/mL xylene solution for type II films, and 0.25 mg/mL chloroform solution of PHT/1-dodecanol (3:1 molar ratio) for type III films. Typically, films were compressed immediately after the addition of solvents. The surface pressure vs mean monomer area isotherms were measured on a Wilhelmy film balance at 20 °C with a compression speed of 30 cm²/min. Multilayers were built up by horizontal deposition on hydrophobic substrates. Silicon and glass substrates were made hydrophobic according to the procedure by Sagiv.⁶³

The LB films deposited on hydrophobic glass cover slips were used for UV-visible absorption, which were recorded on a Hewlett-Packard 8452A diode array spectrophotometer. X-ray diffraction measurements were performed on LB films deposited on hydrophobic silicon wafers at a scanning rate of 0.4° 2 θ /step by Philips X-ray diffractometer. For reflectance infrared studies, glass slides covered with gold from sputter-coating were used as substrates and mounted on a Spectra-Tech reflectance IR unit. The incident beam was 85° to the normal of the substrate surface and IR spectra were collected from 256 scans at a resolution of 4 cm⁻¹ by a Nicolet-730 system.

The transistor device structure is shown in Figure 9. The n-doped Si substrate, with gold contact, functions as the gate, and an oxide layer of 3000 Å is the gate dielectric having a capacitance per unit area of 10 nF/cm². The drain and source electrodes were vacuum deposited using a shadow mask. These electrodes have widths $W = 150$ μ m and channel lengths $L = 100$ μ m. The electric characteristics of these devices were measured under vacuum unless otherwise specified. The current-voltage characteristics were obtained with a Hewlett-Packard (HP) 4145B parameter analyzer. Electron microscopy and diffraction was conducted at 100 KV on C-coated films that had been shadowed with Pt at tan (11/2) to increase contrast.

Results

The formation of a RR-PHT film at the air-water interface was very sensitive to preparation conditions such as spreading solvents and concentrations. The use of concentrated solutions often led to aggregations during spreading and the resulting films were visibly inhomogeneous and rigid. For example, Figure 1 shows the isotherms of films prepared with chloroform as the solvent at different concentrations. Compared with the film obtained from a dilute solution (0.25 mg/mL, film 1), the film spread from a concentrated solution (0.5 mg/mL, film 2) has a lower compressibility and a more drastic transition from an expanded state to a condensed state. More dramatically, the mean monomer area of each thiophene unit in film 2 is only half that of film 1, suggesting that film 2 was twice as thick as film 1. This is consistent with the observation that films prepared from a more concentrated solution appear darker than those prepared from a dilute one. This concentration effect is apparently induced by the strong intermolecular association between

(51) Paloheimo, J.; Stubb, H.; Yli-Lahti, P.; Dyreklev, P.; Inganas, O. *Thin Solid Films* **1992**, 210–211, 283.

(52) Paloheimo, J. *Acta Polytechnica Scandinavica Electrical Engineering Series* **1993**, 75, 2.

(53) McCullough, R. D. *Adv. Mater.* **1998**, 10, 93.

(54) Yai-Lahti, P.; Punkka, E.; Stubb, H.; Kuivalainen, P. *Thin Solid Films* **1989**, 179, 221.

(55) Watanabe, I.; Hong, K.; Rubner, M. F. *Langmuir* **1990**, 6, 1164.

(56) Bao, Z.; Dodabalapur, A.; Lovinger, A. J. *Appl. Phys. Lett.* **1996**, 69, 4108.

(57) McCullough, R. D.; Tristram-Nagle, S.; Williams, S. P.; Lowe, R. D.; Jayaraman, M. *J. Am. Chem. Soc.* **1993**, 115, 4910.

(58) McCullough, R. D.; Lowe, R. D.; Jayaraman, M.; Anderson, D. *J. Org. Chem.* **1993**, 58, 904.

(59) Chen, T.-A.; Wu, X.; Rieke, R. *J. Am. Chem. Soc.* **1995**, 117, 233.

(60) Guillerez, S.; Bidan, G. *Synth. Metals* **1998**, 93, 123.

(61) Yue, S.; Berry, G. C.; McCullough, R. D. *Macromolecules* **1996**, 29, 933.

(62) Ochiai, K.; Tabuchi, Y.; Rikukawa, M.; Sanui, K.; Ogata, N. *Thin Solid Films* **1998**, 327–329, 454.

(63) Dodabalapur, A.; Torsi, L.; Katz, H. E. *Science* **1995**, 268, 270.

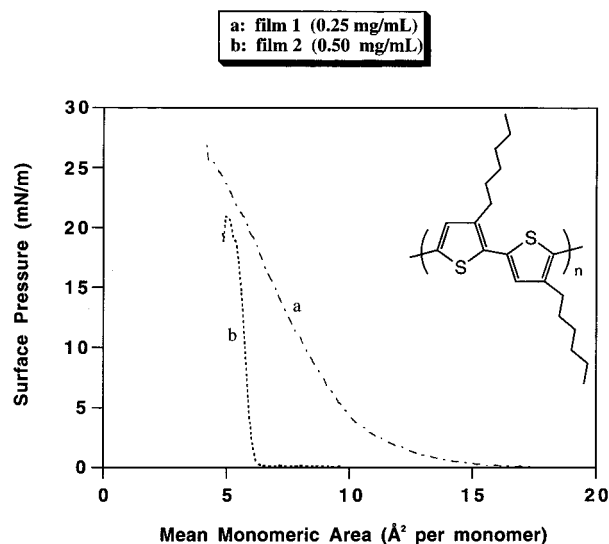


Figure 1. Isotherms of surface pressure and mean monomeric area of RR-PHT spread from chloroform solution with concentrations of 0.5 mg/mL (a) and 0.25 mg/mL (b) at room temperature.

the polymer chains. A similar concentration effect was also observed when other solvents, such as the xylene mixture, were used.

Three types of films have been prepared from the following different solutions: chloroform solution (type I film), xylene solution (type II film), and a mixed solution of dodecanol and chloroform (type III film). In the preparation of type I film, it was observed that during the addition of chloroform solution to the water surface, later additions usually caused a visible disturbance to the previously formed film. After the evaporation of chloroform, an inhomogeneous film (type I) was formed with pink-purple islands separated by blank open water areas, which could be eliminated by subsequently compressing the film with a barrier. The resulting film was stable at surface pressures up to ~ 20 mN/m (Figure 3). The inhomogeneity of the film was presumably caused by a random aggregation, which was expedited by the rapid evaporation of chloroform. To minimize this adverse effect, a less evasive solvent (xylene) was used to yield a more homogeneous film (type II film). The type II film appeared blue-purple and its maximum absorption had a red shift relative to the type I film in the UV-visible region (Figure 2), indicating a more ordered structure.^{53,58} However, the films thus formed were rigid and stiff, rendering them less viable for further manipulation by the trough barrier.

To produce homogeneous and more flexible films, we introduced a water soluble amphiphile as an extractable spread-aiding component into the RR-PHT chloroform solution. Simple amphiphilic molecules with a short hydrophobic chain, such as 1-dodecanol, can form a monolayer at the air/water interface. But, this monolayer is unstable and will quickly dissolve into the subphase.⁶⁴⁻⁶⁶ This dual behavior enables 1-dodecanol to act as a carrier and molecular lubricant for RR-PHT to form more fluid surface films. Initially, 1-dodecanol was cospread with RR-PHT and a macroscopically homogeneous film was formed. Then, 1-dodecanol gradually detached from the film and submerged into the bulk of the subphase as the barrier started compressing the film.

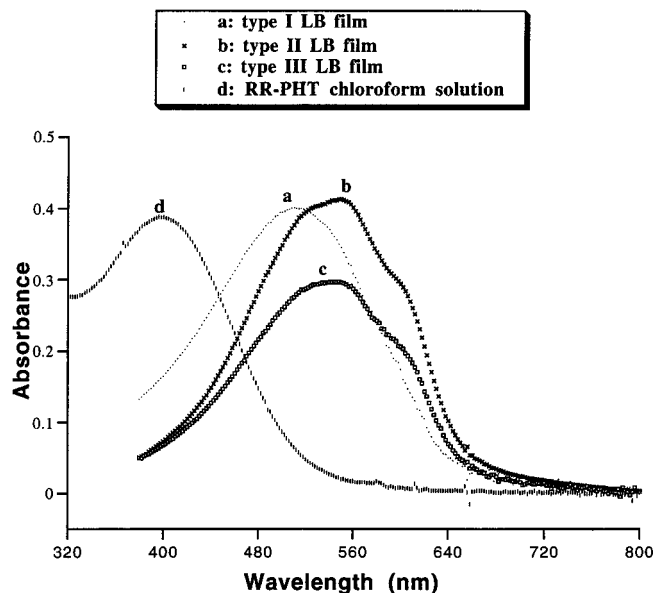


Figure 2. UV-visible absorption spectra of RR-PHT LB films prepared from three different methods: (a) type I film, from chloroform; (b) type II film, from xylene; (c) type III film, from chloroform/dodecanol; and (d) shows the UV-visible absorption spectrum of RR-PHT in chloroform.

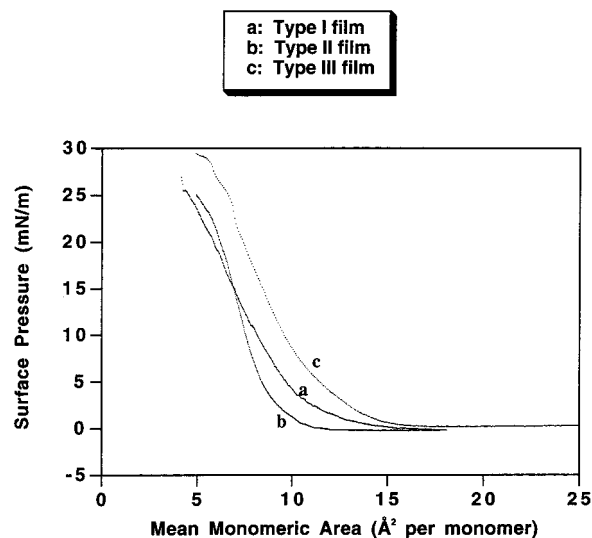


Figure 3. Isotherms of surface pressure and mean monomeric area of RR-PHT prepared by three different methods: (a) type I film, from chloroform; (b) type II film, from xylene; and (c) type III film, from dodecanol/chloroform.

As the lubricant disappeared, polymer chains came closer to each other and started aligning preferentially parallel to the barrier, in response to the compression pressure. Maintaining the surface pressure at 20 mN/m for about half an hour eventually drove the residual 1-dodecanol off the film. This was indicated by the zero net movement of the barrier over time at a fixed pressure. The resulting film (type III film) appeared remarkably homogeneous and showed a bluish purple color similar to that of the type II film.

The surface pressure isotherms of the above three types of films are summarized in Figure 3. Clearly, all three methods yielded stable Langmuir films, which remained stable at a surface pressure higher than ~ 20 mN/m. As judged from the isotherms, the type II film had the lowest compressibility, and hence was the most rigid of the three types. The averaged area occupied by each thiophene unit

(64) MacRitchie, F. J. *Colloid Interface Sci.* **1985**, *107*, 276.

(65) Keyser, P. D.; Joos, P. J. *Colloid Interface Sci.* **1983**, *91*.

(66) Seimiya, T.; Ohbu, K.; Nakamura, A.; Sasaki, T. *Bull. Chem. Soc. Jpn.* **1971**, *44*, 2918.

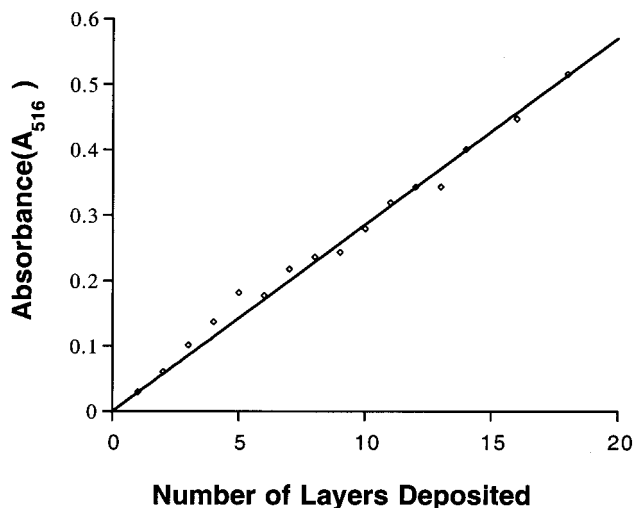


Figure 4. The UV-visible absorbance of type I film as a function of the number of layers deposited, monitored at 516 nm.

at the air-water interface (mean monomer area),^{67,68} was also the smallest for type II film ($\sim 9 \text{ \AA}^2$). The type I film had a larger mean monomer area ($\sim 10.5 \text{ \AA}^2$) and the type III film had the largest one ($\sim 12 \text{ \AA}^2$). As a comparison, the mean monomer area reported for regiorandom PHT is around 5 \AA^2 .⁵⁵ Computer modeling by the CAChe program showed that each thiophene unit should occupy a surface area of 14.5 \AA^2 for a close packed monolayer, assuming the main polymer chain was parallel to the air/water interface with thiophene rings standing vertically. Therefore, the measured monomer areas among three type of films suggest that the type III film has a structure that is closest to a true monolayer.

All three types of films did not adhere well to substrates during vertical deposition, but were readily picked up on hydrophobic substrates by horizontal deposition,⁶⁷ which is also known as Langmuir-Schaeffer deposition, at a transfer ratio of nearly unity up to more than 10 layers. The deposition was monitored by optical absorption. For instance, Figure 4 shows an almost linear relation between the optical absorbance of the film at 524 nm and the number of layers deposited for type I films, indicating that the films were built up uniformly into multilayer structure.^{55,69} The UV-visible spectra of the three types of films deposited on hydrophobic glass substrates are compared in Figure 2. The absorption of the type I film contains very few features and exhibits a single absorption around 520 nm for the $\pi-\pi^*$ transition. By contrast, the spectra of both type II and type III films are red-shifted and both have maximum absorption at 555 nm and a shoulder around 610 nm, which is very similar to the spectrum of cast RR-PHT film that has a well ordered structure and a long conjugation length.⁵⁸ This implies that the structure of both the type II film and the type III film is close to a well-ordered two-dimensional solid, while the type I film is less ordered.

The structure of the films were further investigated by X-ray diffraction studies on multilayer samples prepared on hydrophobic silicon substrates and the results are shown in Figure 5. The (100) Bragg diffraction peaks seen in all the samples indicate the existence of an ordered

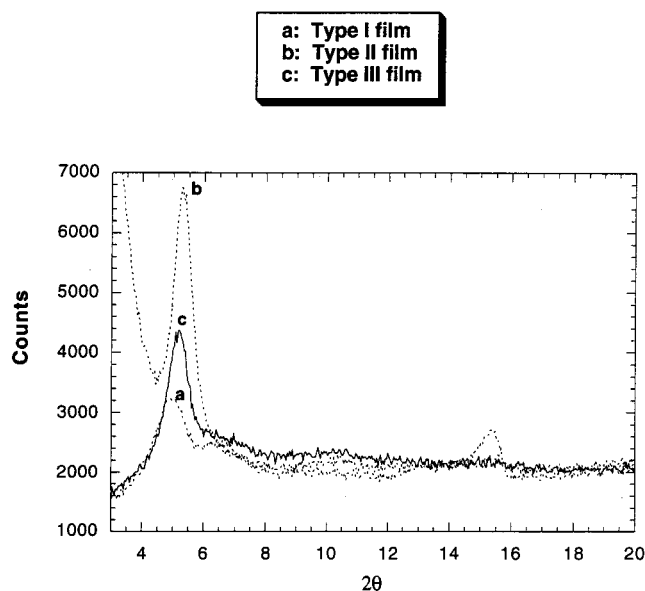


Figure 5. X-ray diffraction patterns of the three types of RR-PHT LB films: (a) type I film, (b) type II film, and (c) type III film.

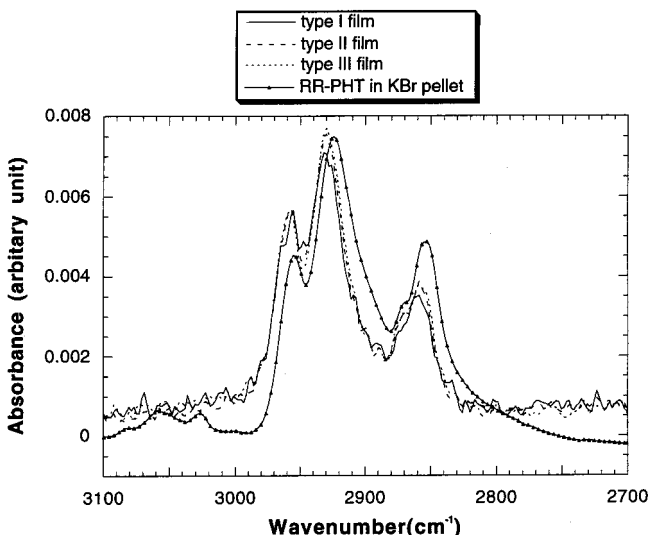


Figure 6. Reflectance absorption infrared spectra of type I (solid line with triangle marks), type II (dashed line), and type III (dotted line) LB films and transmission absorption infrared spectrum of bulk RR-PHT in KBr pellet (solid line).

layer structure parallel to the substrate in all the films.⁷⁰⁻⁷² This is consistent with the previous observation that a uniform transfer of the surface films into supported multilayers has been achieved.^{33,73} The interlayer spacing ($\sim 17 \text{ \AA}$) obtained from (100) diffraction indicated that the polymers had an edge-on conformation with backbones parallel to the substrates.⁵⁶ However, the (100) diffraction peaks in the type II film and the type III film are sharper than that of the type I film, suggesting a longer coherence length, and therefore a better structural ordering along the direction of surface normal in type II and type III films. This agrees with the UV-visible results, which also predicted a better structural ordering in type II and type

(67) Logsdon, P. B.; Pflieger, J.; Prasad, P. N. *Synth. Metals* **1988**, *26*, 369.

(68) Bolognesi, A.; Bertini, F.; Bajo, G.; Provasoli, A.; Villa, D.; Ahumada, O. *Thin Solid Films* **1996**, *289*, 129.

(69) Kurata, T.; Tsumura, A.; Fuchigami, H.; Kozuka, H. *J. Phys. Chem.* **1991**, *95*, 8831.

(70) Winokur, M. J.; Wamsley, P.; Moulton, J.; Smith, P.; Heeger, A. *J. Macromolecules* **1991**, *24*, 3812.

(71) Prosa, T. J.; Winokur, M. J.; Moulton, J.; Smith, P.; Heeger, A. *J. Macromolecules* **1992**, *25*, 4364.

(72) Chen, S.-A.; Ni, J.-M. *Macromolecules* **1992**, *25*, 6081.

(73) Sagisaka, S.; Ando, M.; Iyoda, T.; Shimidzu, T. *Thin Solid Films* **1993**, *230*.

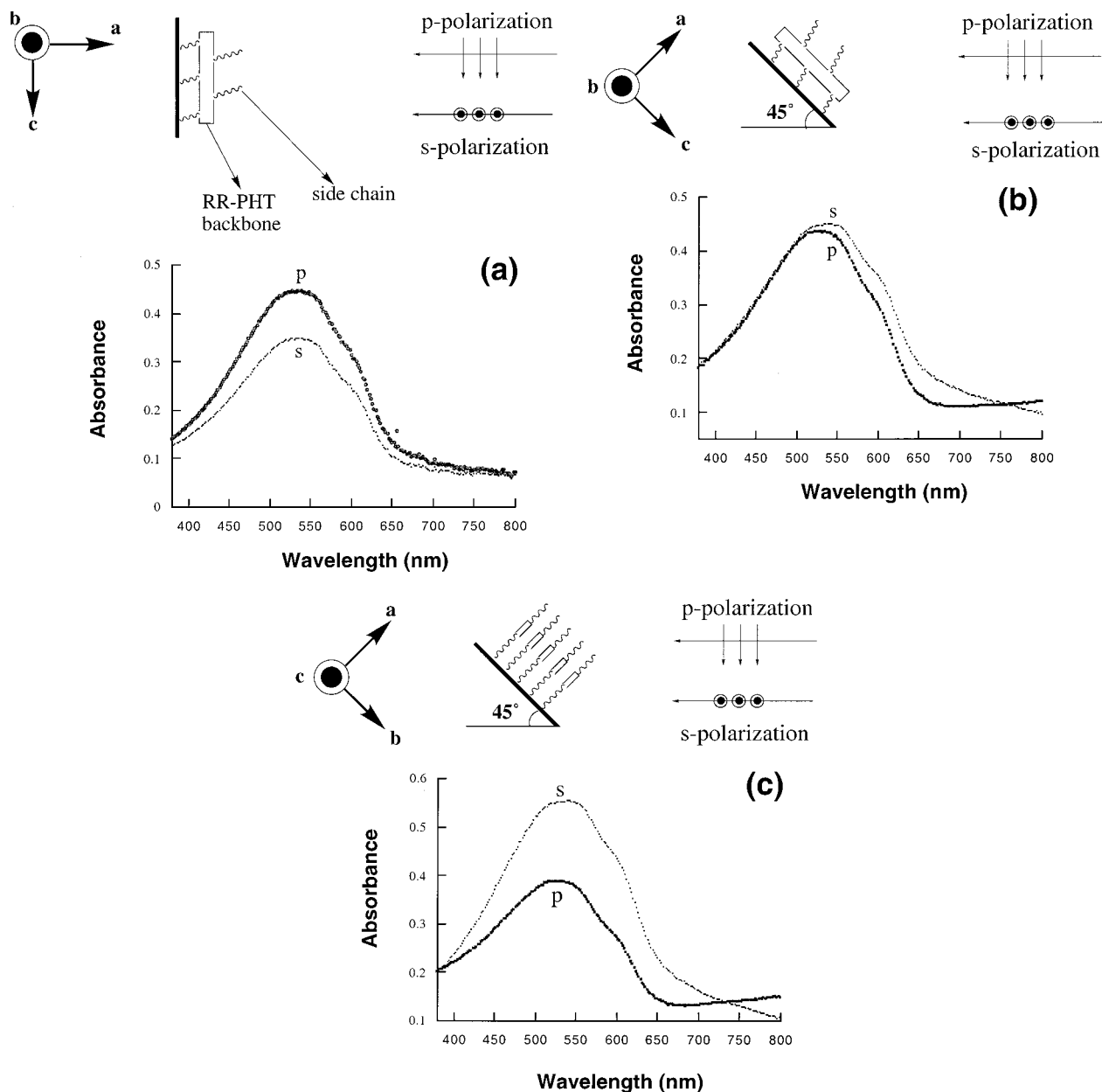


Figure 7. Polarized UV-visible absorption spectra of the type III LB film in different positions relative to the incident beam.

III films. The interlayer distances of the films as calculated from the positions of their (100) peaks are 17.8 (type I film), 16.7 (type II film), and 17.1 Å (type III) film, slightly larger than that of close-packed crystalline RR-PHTs in bulk (16.0–16.7 Å).^{53,59} Since the increase of interlayer distances is likely due to disorders in side chains, the results suggest that the side chains in these films are less well-ordered than in bulk crystalline RR-PHT.

The conformation of the side chains was verified by reflectance infrared spectroscopy. Figure 6 displays the spectra of the three types of films in the high-frequency region (2600–3200 cm^{-1}), which feature the C–H stretching from CH_3 and CH_2 groups in the side chains. The spectrum of bulk RR-PHT in a KBr pellet is also included as the reference for an isotropic and crystalline sample. All the spectra were normalized for comparison and the peaks were assigned as follows:^{74,75} CH_3 asymmetric stretching ($\nu_a(\text{CH}_3)$, 2960 cm^{-1}), CH_2 asymmetric stretch-

ing ($\nu_a(\text{CH}_2)$, 2930 cm^{-1}), CH_3 symmetric stretching ($\nu_s(\text{CH}_3)$, 2870 cm^{-1} , as a shoulder), and CH_2 symmetric stretching ($\nu_s(\text{CH}_2)$, 2858 cm^{-1}). Both the positions and the relative intensities of these peaks appear almost identical in all the films, suggesting that the side chain conformations are very similar, especially in type II and type III films. However, compared with the bulk crystalline sample, the peak positions of both the $\nu_a(\text{CH}_2)$ and the $\nu_s(\text{CH}_2)$ stretching of the films are blue shifted. The blue shift of CH_2 stretching vibrations indicates the existence of disorders in hydrocarbon chains.^{76,77} Therefore, the side chains in all the LB films are less ordered than those of the bulk crystalline RR-PHT, which is often due to the existence of gauche conformation defects.⁷⁸ This is not unexpected, given the short length of the hexyl side chain.⁷⁶

(76) Tao, Y.-T. *J. Am. Chem. Soc.* **1993**, *115*, 4350.

(77) Snyder, R. G.; Strauss, H. L.; Elliger, C. A. *J. Phys. Chem.* **1982**, *86*, 5145.

(78) Laibinis, P. E.; Whitesides, G. M.; Allara, D. L.; Tao, Y.-T.; Parikh, A. N.; Nuzzo, R. *J. Am. Chem. Soc.* **1991**, *113*, 7152.

(74) Watanabe, I.; Cheung, J. H.; Rubner, M. F. *J. Phys. Chem.* **1990**, *94*, 8715.

(75) Parikh, A. N.; Allara, D. L. *J. Chem. Phys.* **1992**, *96*, 927.

Table 1. Dichroic Ratios and Order Parameters of Films Prepared under Different Conditions, Based on Polarized UV-Visible Absorption

film	dichroic ratio (R) ^a	order parameter (O) ^b
LB film type I	1.24	0.07
LB film type II	1.10	0.03
LB film type III	1.60	0.17
cast film	1.01	0
spin-coated film	1.00	0

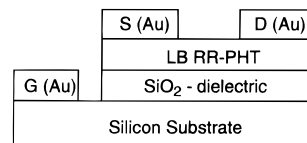
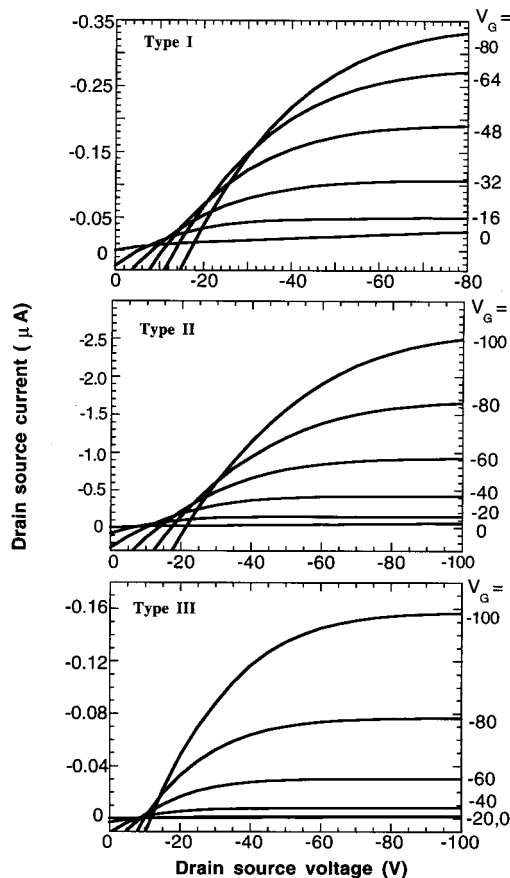
^a R is defined as the ratio of p-polarized absorption to s-polarized absorption in the geometry depicted in Figure 7a. ^b O is defined as $(R - 1)/(R + 2)$. See also ref 80.

The result also agrees with the conclusions drawn from the X-ray diffraction data.

The UV-visible absorption of conjugated polymers from the π - π^* transition is very sensitive to the direction of the polarization of an incident light, which enables the use of polarized light to probe the structural anisotropy within the films.⁷⁹ Figure 7a illustrates the orientation of a type III film relative to different polarization directions and the corresponding spectra. P-polarization is defined so that the electrical field is parallel to the substrate edge that is parallel to the trough barrier during the film deposition (c -axis). S-polarization is orthogonal to p-polarization. The absorption under the p-polarization mode is the strongest, while that under the s-polarization mode is the weakest. The absorption at any other polarization angle falls between these two extremes. Since the absorption of UV light is the strongest when the electric vector of the incident light is parallel to the backbone of a conjugated polymer,^{68,80} the results indicate that the RR-PHT backbones preferentially align parallel to the trough barrier. Obviously, this alignment is induced by the pressure generated from the barrier compression. Further investigations of the polarized absorption spectra by manipulating the geometrical relationship between the film and the electrical field also confirmed the polymer orientation within the film. For example, when the film was tilted 45° away from its original position as in Figure 7a, the difference between the p-polarized and s-polarized absorption diminished (Figure 7b); But when a further 90° in-plane rotation of the film was performed, the difference was again apparent (Figure 7c). These observations again confirm the preferential order and edge-on arrangement of the polymer backbones in the film.⁷⁹

Similar phenomena were seen for type I and type II films, but to a much smaller extent. To compare the preferential order of the backbone of the films, we calculate their dichroic ratio (R) and order parameter (O) and the results are listed in Table 1. Apparently, the polymer backbones in type III films had a better in-plane orientation than those in either type I films or type II films. This may be explained by the formation of domains in type I and type II films before compressing, due to the strong intermolecular aggregation and the lack of fluidity in these films. In the case of the type III film, the introduction of extractable amphiphiles reduced the aggregation, increased the film fluidity, and improved the processability and the in-plane ordering of an otherwise stiff film. In a control experiment, a film cast from the same solution that was used for preparing the type III film showed identical absorption, regardless of the polarization direction (Figure 8). Spin-coated films also showed no dichroism.

The LB films were subsequently made into field-effect transistor devices to test their charge-carrier mobility (μ).

**Figure 8.** Schematic structure of a field-effect transistor fabricated from LB films of RR-PHT. G: gate; S: source; D: drain.**Figure 9.** Current-voltage characteristics of transistors prepared from RR-PHT LB films (5 layers): type I, type II, and type III.

The cross-sectional view of the transistor device structure is shown in Figure 8 and its preparation has been previously described.⁵⁶ Figure 9 shows typical I-V curves acquired from devices operating in the accumulation mode. The drain-source currents (I_{DS}) of negative sign scale-up with negative gate voltages (V_G). At the saturated region, I_{DS} can be described using eq 1, where μ is the field-effect mobility, W is the channel width, L is the channel length, and C_i is the capacitance per unit area of the insulating layer (SiO_2 , 3000 Å, $C_i = 10 \text{ nF/cm}^2$). A plot of $I_{DS}^{1/2}$ vs V_G can be used to obtain V_0 , the extrapolated threshold voltage, after extrapolation to the V_G axis. The field-effect mobility can then be calculated from eq 1.

$$I_{DS} = \frac{WC_i}{2L} \mu (V_G - V_0)^2 \quad (1)$$

The average of the best values of field-effect mobility measured for each type of film was $2 \times 10^{-2} \text{ cm}^2 \text{ V}^{-1} \text{ s}^{-1}$ for the type II film, $6 \times 10^{-3} \text{ cm}^2 \text{ V}^{-1} \text{ s}^{-1}$ for the type I film, and $3 \times 10^{-3} \text{ cm}^2 \text{ V}^{-1} \text{ s}^{-1}$ for the type III film. The mobility of the type II film is among the highest of organic thin film transistors produced by LB techniques. Given the structural similarity of type II and type III films, the

(79) Rikukawa, M.; Rubner, M. F. *Langmuir* **1994**, *10*.

(80) Kani, R.; Nakano, Y.; Majima, Y.; Hayase, S.; Yuan, C.-H.; West, R. *Macromolecules* **1994**, *27*, 1911.

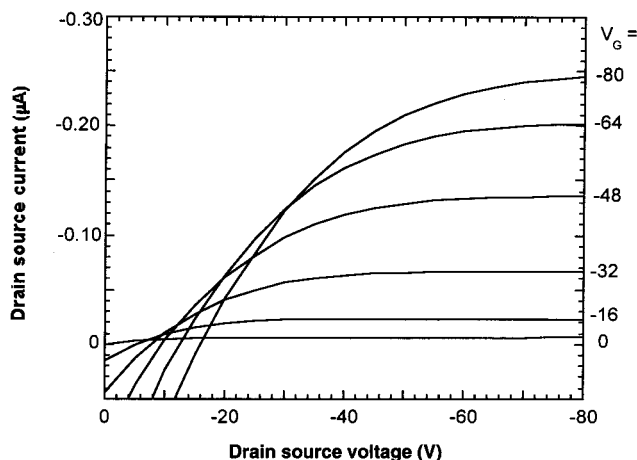


Figure 10. Current–voltage characteristics of transistors prepared from a 2-layer type I LB film.

relatively low mobility of the type III film is unexpected. A possible explanation is that the electrical properties are dominated by defects or impurities within the films rather than the intrinsic electrical activity of the polymers. This was indeed verified by the existence of nanometer size pinholes in type III film under the examination of a transmission electron microscope, while such defects were not spotted in either the type I or the type II film (data not shown). The defects in the type III film were either residual dodecanol or cavities formed when dodecanol dissolved before the rigid polymer coalesced. In contrast to the preferential order detected by the polarized UV–Vis absorption, no significant anisotropic mobility was measured in the films. The apparent contradiction can also be explained by the presence of the defects. The mobility of the devices was insensitive to the thickness of the films. Devices composed of two to five layers had very similar mobility that was higher than that of a single layer device (Figure 10). The result suggested that the charge carriers were mostly confined within the first few molecular layers of the film and similar results have been observed for other organic field-effect transistors.⁶³

Discussion

Solution methods such as casting and spin-coating are often used to prepare soluble organic thin films.⁵⁶ In the case of RR–PHT, thin films prepared by spin-coating usually displayed relatively low field transistor mobility ($\sim 10^{-3} \text{ cm}^2 \text{ V}^{-1} \text{ s}^{-1}$) while films prepared by casting RR–PHT chloroform solution onto Si/SiO₂ showed high mobilities similar to that of the type II film in this study. Although the solution cast procedure has the advantages of easy operation and low cost, it is very difficult to control the thickness, thickness uniformity, smoothness, and molecular orientation. Most of these can, however, be easily controlled by LB techniques through the layer-by-layer deposition process. The absolute thickness of each layer was not determined in this study, but it can be estimated from the isotherm and the X-ray diffraction results. For instance, the monomeric area of the type II film obtained from the isotherm is about half of that expected from the close packing model, which suggests a Langmuir film containing a double layer. The formation of a double layer is in fact a characteristic of Langmuir films formed by many other rodlike polymers.² Considering the interlayer spacing (16.7 Å) obtained from X-ray diffraction, the thickness of each Langmuir film is therefore 33.4 Å. A device that contains 5 to 10 layers will have a thickness of 160–330 Å. Compared with cast films, which are usually 10^3 – 10^4 Å thick, the LB film is ultrathin.

Although the anisotropy was not detected in the electrical measurements, the polarized visible spectra did show preferential alignment of the polymer backbones within the LB films, which did not exist in cast films. The use of dodecanol as an extractable agent for delivering the polymer succeeded in preventing premature aggregation and providing effective molecular lubrication. However, the charge carrier transporting ability of the type III film was reduced by pinholes in the film. The formation of those defects could be due to some local phase separation processes.⁵⁵ To reduce or eliminate the phase separation, water soluble amphiphiles with better miscibility with the polymer may be used. For example, the hydrophobic part of the soluble surfactant may be modified to increase the compatibility with the active component. The hydrophilic part can also be modified to adjust the solubility. For example, changing the hydroxyl group to a carboxylic group will change the solubility and enable the control of dissolving by pH. The subphase and the temperature are also tunable for optimal conditions. Since the dissolution of amphiphiles is a function of time and surface pressure, the rate at which a film is compressed is also an influential parameter. Overall, the spreading-then-extracting method provides a flexible alternative to manipulate polymer films which have little or no amphiphilicity. The macroscopic homogeneity and the optical isotropy of films prepared by this method may also be useful for constructing thin film photonic devices.

The challenge of fabricating RR–PHT thin film devices by LB techniques is to transfer films with vertical deposition while preserving their good electrical properties. Vertical depositions can be realized by doping polymers with long chain fatty acids. But, as mentioned earlier and also witnessed in this work, defects in films, in the form of either impurities or cavities, are detrimental to the electrical properties, let alone the fact that films thus made are usually unstable and the polymer chains are randomly oriented. A better approach is perhaps to modify the molecular structure of polythiophenes to render them amphiphilic. Callender et al. replaced alkyl side chains with alkoxy side chains and were able to vertically deposit multilayer films, in which the macromolecules were completely disordered.⁸¹ Amphiphilic polythiophene with long hydrocarbon chains was also synthesized and deposited onto hydrophobic substrates by vertical transfer, during which the structural order of surface films were also lost.⁷³ More recently, Bolognesi et al.^{68,82–84} attached various hydrophilic groups to the ends of side chains and a centipede-like conformation was presumably adopted by the polymers at the air–water interface. Transfer ratios close to unity were reported in both Y-type and Z-type depositions and preferential alignment of the polymer backbones along the dipping direction was also observed. But, because the bending of the side chains caused thiophene ring twisting away from a coplanar conformation, the conjugation of the backbones was far less effective than that of regioregular PAT. An ideal structure for an amphiphilic polythiophene would be one with a regioregular conformation that has an alternating arrangement of hydrophobic and hydrophilic side chains, as has recently

(81) Callender, C. L.; Carere, C. A.; Daoust, G.; Leclerc, M. *Thin Solid Films* **1991**, *204*, 451.

(82) Bolognesi, A.; Bajo, G.; Geng, Z.; Porzio, W.; Speroni, F. *Thin Solid Films* **1994**, *243*, 683.

(83) Belobrzeczkaja, L.; Bajo, G.; Bolognesi, A.; Catellani, M. *Synth. Metals* **1997**, *84*, 195.

(84) Bolognesi, A.; Bajo, G.; Paloheimo, J.; Ostergard, T.; Stubb, H. *Adv. Mater.* **1997**, *9*, 121.

been reported by McCullough and colleagues.⁸⁵ The overall structure of such a polymer has one-half of the side chains staying in the water while the other half stay in the air, thus providing a suitable amphiphilicity while preserving a high degree of conjugation that is essential for electrical and optical quality. Conducting nanowires have been made from these amphiphilic thiophenes by LB techniques.⁸⁵

Conclusions

We investigated and compared different methods of making pure ultrathin Langmuir-Blodgett films from regioregular poly(3-hexylthiophene). In all the cases, stable surface films were formed and horizontally depos-

(85) Bjornholm, T.; Greve, D. R.; Reitzel, N.; Hassenkam, T.; Kjaer, K.; Howes, P. B.; Larsen, N.; Bogelund, J.; Jayaraman, M.; Ewbank, P. C.; McCullough, R. D. *J. Am. Chem. Soc.* **1998**, *120*.

ited into multilayers with ordered lamella structures. The polymer backbones were found to be parallel to the substrates with an edge-on conformation. High field-effect mobility was obtained from films prepared by using xylene as the spreading solvent. Films prepared by the dodecanol-extracting method displayed considerable in-plane orientation. We believe the soluble-amphiphile-extracting method provides a flexible alternative to manipulate unconventional Langmuir films.

Acknowledgment. Support of this research by the National Science Foundation (J.T.G.) is gratefully acknowledged. The authors thank Dr. Andrew Lovinger and Ms. Joyce Sapjeta for assistance in TEM and AFM characterizations.

LA9904455